Spectral diffusion and its influence on the emission linewidths of site-controlled GaN nanowire quantum dots

M. Holmes,[1,*] S. Kako,[2] K. Choi,[1] M. Arita,[1] and Y. Arakawa[1,2,†]

[1]*Institute for Nano Quantum Information Electronics, The University of Tokyo, 4-6-1 Komaba, Meguro-ku, Tokyo 153-8505, Japan*

[2]*Institute of Industrial Science, The University of Tokyo, 4-6-1 Komaba, Meguro-ku, Tokyo 153-8505, Japan*

(Received 20 August 2015; published 30 September 2015)

Fourier transform spectroscopy is used to determine/control the degree of spectral diffusion in high-quality site-controlled GaN nanowire quantum dots. Detailed analysis, including the development of a statistical model and Monte Carlo simulations, provides evidence that the broadening is caused by photoinduced excitation of defects. Furthermore, performing the experiment under weak excitation allows for an estimate of the homogeneous linewidth to be made (135 μeV). The origins of this linewidth are discussed, and the existence of an alternate dephasing mechanism is inferred. A limit on the emission linewidth at zero excitation is also discussed.

DOI: 10.1103/PhysRevB.92.115447 PACS number(s): 81.07.Ta, 81.07.Gf, 78.55.Cr

I. INTRODUCTION

The emission linewidths of optical transitions in semiconductor nanostructures are important measures of coherence, and they are also indicators of the degree to which interactions with the environment are occurring, be they interactions with material vibrations, electronic fluctuations, or the modes of optical resonators. Spectral diffusion is one such linewidth-limiting phenomenon, whereby an optical transition between two states in a nanostructure undergoes inhomogeneous linewidth broadening through Coulomb interactions with the fluctuating electronic environment. The exact degree to which spectral diffusion will occur in a given situation depends on several factors, such as the quality of the material, the interaction strength, and even the time scale on which the fluctuations occur [1]. Being a limiting factor for the generation of indistinguishable photons [2], spectral diffusion is an important topic that demands thorough analysis.

To date, there have been many observations of this effect in semiconductor nanostructures made from a range of materials [3–5]. In particular, polar III-nitride quantum dots (QDs), which exhibit large interaction strengths due to their internal-field-induced exciton permanent dipole moments [6,7] and relatively large densities of surrounding defects, tend to have large inhomogeneous linewidths that can reach up to 10's of meV for single quantum transitions [8–10] even at cryogenic temperatures where other broadening mechanisms, such as the interaction with acoustic phonons, are suppressed. Although it has been shown that smaller QDs exhibit smaller permanent dipole moments, resulting in narrower inhomogeneously broadened emission linewidths [11], these linewidths still tend to be of order $\sim$1 meV, rendering the emission of indistinguishable photons all but impossible.

Even though there have been no experimental studies on the extent of spectral diffusion in nitride nanowire QDs to date, it is anticipated that the use of nanowire structures to localize the QDs will alleviate the spectral diffusion problem to some degree by a combination of several effects, such as the following:

(i) The fact that nanowires tend to exhibit high-quality material with fewer structural defects, suggesting a somewhat cleaner environment.

(ii) The growth mode of dots in nanowires is not strain-limited, allowing for the formation of smaller dots that will exhibit smaller interaction strengths.

(iii) The volume of the environment is physically reduced in nanowires (with the caveat that surface environments are closer to the dot).

Here we investigate the spectral diffusion mechanics in site-controlled GaN/$Al_{0.8}Ga_{0.2}N$ nanowire quantum dots, and we provide experimental evidence, together with a complementary theoretical model, that it can be controlled to some extent. III-nitride semiconductors in general are receiving much attention at present, particularly due to their widespread use in solid-state lighting, and their nanostructures have also been in the spotlight in recent years, with advances being made toward high-temperature operational single-photon sources [12–17], nanowire field-effect [18] and quantum dot single-electron transistors [19], and also the realizations of plasmonic nanowire lasers [20], quantum-well and nanowire polariton lasers [21,22], and QD-based microdisk lasers [23,24]. Nitride-based QDs are also theorized to be useful for various quantum-information-based applications [25,26]. In particular, site-controlled nanowire QD structures [27], such as those used in this study, are of additional interest as they offer the possibility of fabricating structured arrays of devices, a property that will be of significant importance for the manufacture of future devices with real-world applications.

The studied GaN/$Al_{0.8}Ga_{0.2}N$ QDs are located near the tips of site-controlled nanowires grown by metalorganic chemical vapor deposition (MOCVD) [28], and they have been shown recently to possess many favorable optical properties, such as large biexciton binding energies [27], well-defined coherently controllable excited states [29,30], and room-temperature single-photon emission [12]. Figure 1 shows scanning electron microscopy (SEM) images and a schematic of a single device. The dots are typically $\sim$1 nm in height [30] and therefore tend to emit in the deep uv at energies greater than 4 eV, where the energy resolution of spectrometers becomes increasingly worse due to the inverse relationship between wavelength and energy. In the experiments described herein, Fourier

*holmes@iis.u-tokyo.ac.jp

†arakawa@iis.u-tokyo.ac.jp

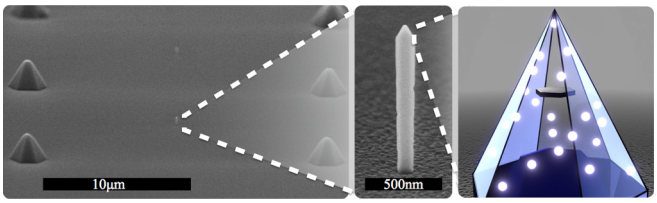

FIG. 1. (Color online) SEM images of a single site-controlled $GaN/Al_{0.8}Ga_{0.2}N$ nanowire quantum dot and position markers. The right image is a simplified schematic of the nanowire tip showing a distribution of charges (glowing balls) in the vicinity of the quantum dot (central hexagonal inclusion).

transform spectroscopy [1,31–34] performed with a home-built piezodriven interferometer operating in the ultraviolet is used to overcome our spectrometer resolution limit and accurately measure the QD emission linewidths in the spectral domain via interference measurements in the temporal domain (the envelope function of the interference decay is related to the emission spectrum via a Fourier transform).

II. EXPERIMENT AND ANALYSIS

We begin by showing some basic optical properties of a nanowire QD selected for this study. The emission spectrum shown in Fig. 2(a) measured using standard microphotoluminescence spectroscopy is limited by the resolution of the experimental setup. The left panel inset shows a time series of collected spectra measured over a period of 300 s (100 spectra, 3 s integration time) revealing that the emission from the QD is temporally stable and that there are no measurable discrete spectral jumps. The right inset shows a histogram of photon coincidence counts measured using the Hanbury-Brown and Twiss (HBT) setup. The data reveal the single-photon nature of the emission by the fact that the value of the second-order coherence function at zero time delay, $g^{(2)}[0]$, is <0.5 (we measure a raw value with no correction of 0.32 ± 0.11). In Fig. 2(b) we show a measurement of the emission lifetime of the decay as measured by time-correlated single-photon counting using one of the photomultiplier tubes (PMTs). The emission from the QD exhibits a monoexponential decay with a lifetime of ∼400 ps, which is consistent with previous studies on small nitride QDs [35] and typical for this kind of GaN/AlGaN nanowire dot. At low temperatures we can assume that this lifetime is the radiative lifetime of the dot, and note that such a lifetime (in the absence of other sources of decoherence) would limit the emission linewidth to be on the order of a few μeV. In reality, however, spectral diffusion will lead to much broader emission linewidths, but as the spectrometer limits the measurement in this case, we utilize Fourier transform spectroscopy to make measurements of the linewidth in the time domain via interference measurements. To perform such experiments, we map the interference fringe contrast, C, measured while tuning the path difference, τ, in a Michelson interferometer. The fringe contrast is defined as

$$C = \frac{(I_{\max} - I_{\min})}{(I_{\max} + I_{\min})}, \tag{1}$$

where $I_{\max}$ and $I_{\min}$ are the maximum and minimum intensities found by fitting the interference patterns with a sinusoid function. The measurements are performed at 4 K through several values of interferometer path delay and over a range of excitation powers using a 266 nm continuous-wave laser (an energy lower than the barrier material band gap). The low and constant temperature is necessary in these experiments to suppress the interaction with phonons, which could also affect the emission linewidth [36,37]. Further experimental details can be found in Sec. VII.

The interference measurements of the emission from a GaN nanowire QD are presented in Fig. 3 (the data are

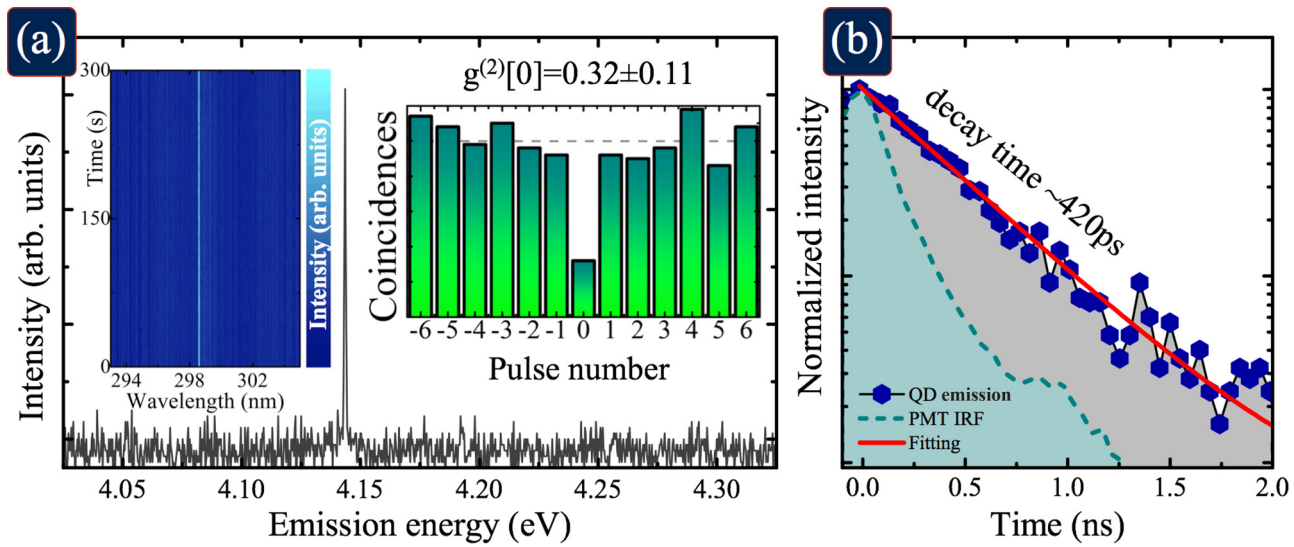

FIG. 2. (Color online) (a) Emission spectra of a site-controlled nanowire quantum dot under excitation at 160 W cm^{-2}. The emission line is limited by the spectral resolution of the experimental setup. The insets show the temporal variation of the emission (i.e., no spectral jumping) and the intensity autocorrelation revealing a $g^{(2)}[0]$ value of 0.32. (b) Measurement of the lifetime of the QD when excited with 200 fs laser pulses (the response function of the photomultiplier tube used for detection is also shown). The decay of the QD emission is monoexponential with a decay time of ∼420 ps.

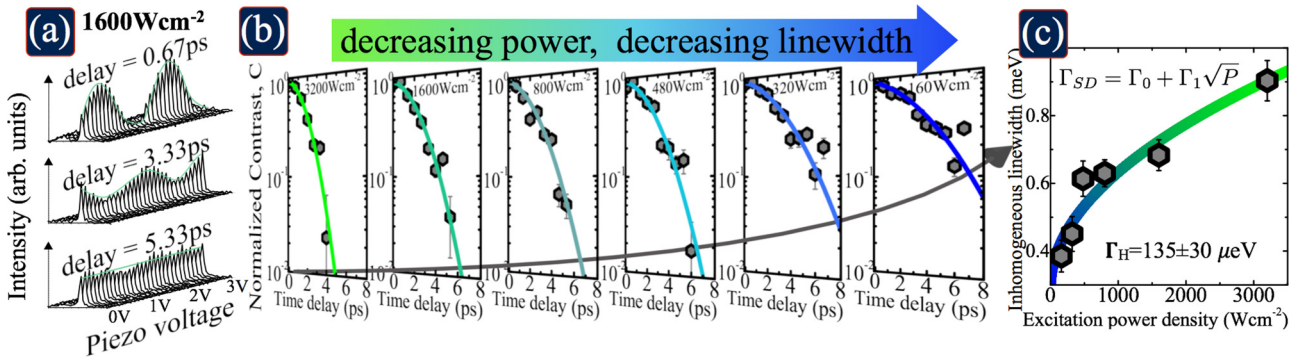

FIG. 3. (Color online) (a) QD emission interferograms measured by fine tuning the piezo arm of the interferometer at various course delays (excitation power density = 1600 W cm^{-2}). (b) A series of semilogarithmic plots showing the decay in fringe contrast as a function of excitation power. The contrast decay is slower at lower excitation powers, indicating a narrowing of the spectral width. The solid lines are fits to the data of Eq. (2). (c) The variation of the inhomogeneous linewidth with excitation power.

taken from the same dot represented in Fig. 2). We observe the expected decay in fringe visibility as the interferometer path difference is increased [shown clearly in Fig. 3(a)], and we find that upon decreasing the excitation power, the fringes remain visible at longer decay times [as shown by the visibility decay plots in Fig. 3(b)]. This indicates a narrowing of the spectral emission line as the excitation power is reduced, revealing a power-dependent nature of the spectral diffusion (SD) process. We envisage the simple situation of a (homogeneously broadened) Lorentzian emission line (of width Γ_H) that is further broadened by power-dependent environment fluctuations, resulting in a Gaussian line shape of width $\Gamma_{\rm SD}$. Consequently, the data are fitted [see the solid lines in Fig. 3(b)] with the Fourier transform of a Voigt function:

$$C(\tau) = \exp\left[-\left(\frac{\tau}{\tau_{\rm SD}}\right)^2 - \left(\frac{\tau}{\tau_H}\right)\right], \qquad (2)$$

from which the linewidths [full width at half-maximum (FWHM)] of the components can be respectively extracted from the fitting via the following relations:

$$\Gamma_{\rm SD} = \frac{2\sqrt{\ln 2}}{\pi\tau_{\rm SD}}, \quad \Gamma_H = \frac{1}{\pi\tau_H}. \qquad (3)$$

By fitting the experimental data consistently, we extract the power dependence of $\Gamma_{\rm SD}$ [shown in Fig. 3(c)] and a homogeneous linewidth of $\Gamma_H = 135 \pm 30\,\mu$eV. Although the error is large, this estimated value of the inhomogeneous linewidth of site-controlled GaN nanowire QDs in the temporal domain is similar to that previously measured directly in the energy domain from self-assembled GaN/AlN QDs [38] using a high-resolution spectrometer. However, we note that it is still much broader than the radiative decay limit, leading us to the conclusion that there must be some other exciton decoherence process occurring (a process that leads in particular to a Lorentzian line shape). We estimate the time scale of this process to be of order 10 ps, and we leave the origin of this as an open question at present, although we suggest that in the case of these nanowire QDs it could possibly be determined by a motionally narrowed diffusion [1] due to the fast fluctuations of itinerant charges on the nanowire surface or in the GaN core region of the nanowire, or perhaps some other, hitherto unknown, process inherent to nitride QDs.

Nevertheless, the fact remains that the emission line is still largely inhomogeneously broadened, and next we turn our attention to the nonlinear increase in the inhomogeneous linewidth with increasing excitation power. We see in Fig. 3(c) that the data are well described with a fitting of the form $\Gamma_{\rm SD} \propto \sqrt{P}$ (with a constant offset), similar to that observed by Empedocles and Bawendi for CdSe nanocrystalline dots [39]. In the following section, we explain this phenomenon in general terms with a statistical model based on the excitation of charges into a distribution of traps near the dot.

III. STATISTICAL MODEL BASED ON THE MULTIVARIATE HYPERGEOMETRIC DISTRIBUTION

We consider the environment of the dot, limiting our analysis to a region in the tip of the nanowire that consists of the QD surrounded by a wide-band-gap barrier of $Al_{0.8}Ga_{0.2}N$ as it is assumed that charge traps in this region, being the closest to the dot, will dominate the spectral diffusion/line broadening mechanism. Now, as is discussed in more depth below, the majority of traps in this region are likely to be deep-level acceptorlike defect complexes [40,41], and even the residual donorlike defects will also become positively charged electron traps by releasing their charge to midband surface states [42,43]. Due to the fact that our excitation laser energy is lower than the $Al_{0.8}Ga_{0.2}N$ band gap, it is not possible to photoexcite carriers directly from the valence continuum to the conduction continuum in this region, and we therefore assume that the traps come to be occupied through either direct photoexcitation from the valence band or by the capture of charges that have been optically liberated from the surface states into the conduction band. The electrons remain trapped for a short time before escaping via either recombination with valence-band holes, tunneling to the surface states, or some other scattering mechanism. For modeling purposes, we define a distribution of N traps in the vicinity of the dot that induce shifts Δ_i when occupied, where i indexes each trap, and we stress that in working through the model here we do not define any specific trap distribution geometry, and therefore we maintain generality for different geometries. We assume that at any given time, n of the N traps are occupied (where n is the steady-state value for the dynamic excitation, photoliberation,

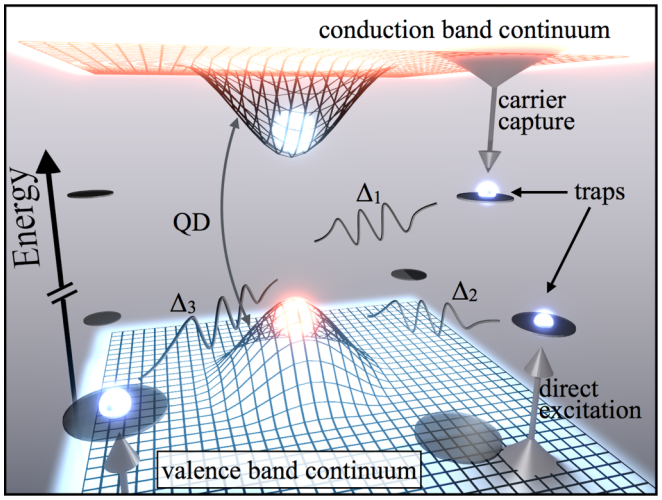

FIG. 4. (Color online) Schematic showing the electronic states in a plane slice through a nanowire QD surrounded by some charge trap localized states. When a trap becomes occupied, it induces a shift Δ_i in the QD emission energy.

and capture processes, and it is dependent on the excitation power P). There are therefore ${}^{N}C_{n}$ possible values of the resulting electric field due to the n trapped electrons, and temporal fluctuations in the field's magnitude and direction (due to different traps being occupied) result in the spectral diffusion. A schematic of the model, showing a slice through the QD, is shown in Fig. 4.

In the framework of the above model, the instantaneous emission energy of the dot can be expressed as

$$E = E_0 + \sum_{i=1}^{N} \Delta_i n_i, \tag{4}$$

where n_i is 1 if the ith trap is occupied and zero if empty ($\sum n_i = n$), and E_0 is the emission energy of the dot in the special case when all traps are empty. Following this definition, the variance in the emission energy due to the possible configurations of the n occupied traps is expressed as

$$\mathrm{var}[E] = \mathrm{var}\left[\sum_{i=1}^{N} \Delta_i n_i\right] \tag{5}$$

$$= \sum_{i=1}^{N} \Delta_i^2 \mathrm{var}[n_i] + \sum_{i\neq j} \Delta_i \Delta_j \mathrm{cov}[n_i, n_j], \tag{6}$$

which can be easily related to the spectral diffusion-limited emission linewidth such that $\Gamma_{\mathrm{SD}} = 2\sqrt{2\ln 2\,\mathrm{var}[E]}$, wherein the assumption is made that the spectral diffusion effect leads to a single Gaussian peak. In effect here we are modeling spectral diffusion as the selection of n balls from an urn containing N different colored balls (with each color uniquely identifying a trap, the selected balls representing the traps that become occupied, and the number of selected balls relating to the excitation power). The statistics of such a situation are dictated by the multivariate hypergeometric distribution, for which the variance and covariance of the occupations of each distinguishable trap can be expressed as [44]

$$\mathrm{var}[n_i] = n\frac{(N-n)}{(N-1)}\frac{1}{N}\left(1-\frac{1}{N}\right), \tag{7}$$

$$\mathrm{cov}[n_i, n_j] = -n\frac{1}{N^2}\frac{(N-n)}{(N-1)}. \tag{8}$$

Upon inserting these relations into Eq. (6), the energy variance can be obtained as a function of the number of excited charges:

$$\mathrm{var}[E] = n\frac{(N-n)}{(N-1)}\left[\sum_{i=1}^{N}\frac{\Delta_i^2}{N}\left(1-\frac{1}{N}\right) - \sum_{i\neq j}\frac{\Delta_i\Delta_j}{N^2}\right]. \tag{9}$$

This can be readily rearranged by collecting together the coefficients of powers of $1/N$ such that

$$\mathrm{var}[E] = n\frac{(N-n)}{(N-1)}\left[\sum_{i=1}^{N}\frac{\Delta_i^2}{N} - \left(\sum_{i=1}^{N}\frac{\Delta_i}{N}\right)^2\right] \tag{10}$$

$$= n\frac{(N-n)}{(N-1)}\mathrm{var}[\Delta], \tag{11}$$

where $\mathrm{var}[\Delta]$ is the variance in shifts per trapped charge of the trap distributions, which depends only on the spatial locations of traps and the exact interaction mechanism with the QD. In the limit that $N \gg 1$, Eq. (11) becomes

$$\mathrm{var}[E] = n\left(1-\frac{n}{N}\right)\mathrm{var}[\Delta], \tag{12}$$

such that the emission linewidth, Γ_{SD}, is proportional to $\sqrt{n}$ for small n, and hence is proportional to the square root of the excitation power under the reasonable assumption that $n \propto P$, in good agreement with the experimental data. This model, therefore, clearly describes the experimentally observed power-dependent spectral diffusion-limited broadening, and we note here again that the model is entirely general in terms of the spatial distribution of traps, with the maximum extent of possible broadening for a given distribution being proportional to $\sqrt{\mathrm{var}[\Delta]}$.

IV. MONTE CARLO SIMULATIONS AND THE CARRIER TRAP DENSITY

Next we show that the value of $\sqrt{\mathrm{var}[\Delta]}$ for a distribution of traps in the vicinity of a QD is reasonable enough to explain the experimentally measured values of Γ_{SD}. To do this, we perform Monte Carlo simulations on randomly generated trap distributions as described in the following. The most common impurity species in nominally undoped III-nitride structures (particularly those grown by MOCVD) are silicon and oxygen, easily having densities [40,45] of order $\rho \sim 1\times10^{18}\,\mathrm{cm}^{-3}$ (Si) and $\rho \sim 1\times10^{19}\,\mathrm{cm}^{-3}$ (O), respectively (equivalent to approximately one atom per 10 000 and one atom per 1000 in the host crystal). There has been much debate in the literature on the exact formation processes of such defects/dopants, particularly with regard to the trap depths. For example, Si has been shown to act as a shallow donor in $\mathrm{Al}_x\mathrm{Ga}_{1-x}\mathrm{N}$ across almost all of the composition range, whereas O undergoes a change to a deep-level trap (DX) for $x \geqslant 0.27$ with an optical ionization energy of $\sim$1.3 eV [40,46].

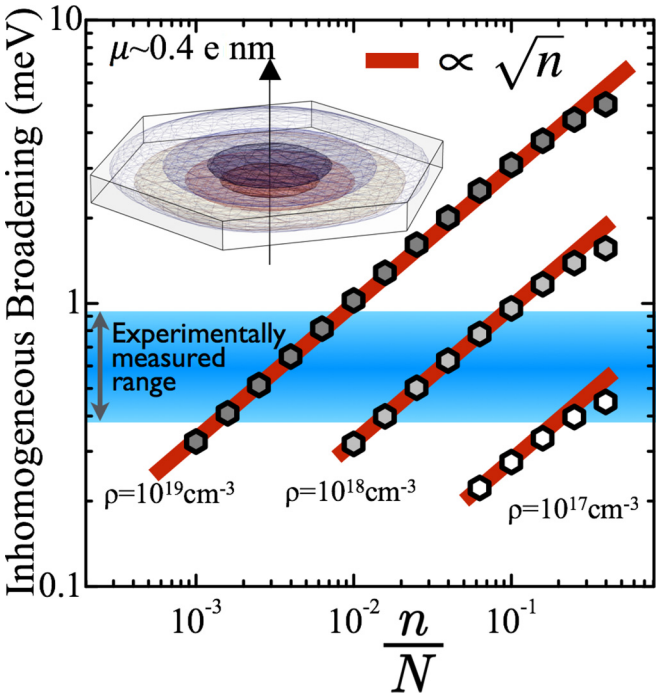

FIG. 5. (Color online) Monte Carlo simulation results showing the dependence of the degree of spectral diffusion on the fraction of occupied traps. The red lines show the expected $\sqrt{n}$ dependence. The inset shows calculated electron (blue) and hole (red) ground-state density functions $\langle\Psi_{e,h}|\Psi_{e,h}\rangle$ for a simulated QD, in this case giving a dipole moment of $\sim 0.4e$ nm. The simulations show that typical trap densities ($\rho = 10^{18}-10^{19}$ cm^{-3}) can explain the experimentally observed linewidth broadening. It can also be seen that densities larger than $\rho = 10^{17}$ are required to adequately explain the measured range of data.

These DX centers are likely to be acceptorlike complexes with cation vacancy centers (V_{III}) in the crystal [41,47], which have also been shown to reach similarly high densities in III-nitrides [48,49]. For simplicity, we assume distributions of generic traps for our simulations, and we ignore the specific effects of surface trapped charges as a first approximation, as the spectral diffusion will be dominated by energy shifts due to the ionization of traps in the body of the nanowire that are close to the dot. We note that it is not necessary to specifically treat a quantum-well-like "wetting layer" that forms during the QD growth [30], as its binary nature suggests a lack of potential fluctuation-related charge traps, and its location ensures that charges trapped specifically in the well will interact relatively weakly with the QD exciton dipole moment.

For simplicity, the trapping of an electron in the ith trap is modeled to induce an electric field at the center of the dot, $\mathbf{F}_i$, and hence an energy shift in the QD emission energy of $\Delta_i = \mu \cdot \mathbf{F}_i$, where μ is the exciton dipole moment and is given by $\mu = \langle\Psi_h|\hat{\mathbf{z}}|\Psi_h\rangle - \langle\Psi_e|\hat{\mathbf{z}}|\Psi_e\rangle$. Here $\Psi_{e,h}$ are the wave functions of the ground-state electron and hole, respectively, which are evaluated with eight-band $k \cdot p$ theory using the NEXTNANO device simulation software [50] to estimate a dipole moment of $\mu \sim 0.4e$ nm for a hexagonal disk shaped GaN/$Al_{0.8}Ga_{0.2}N$ QD emitting at about 4.15 eV (see the inset in Fig. 5). It is also assumed that the magnitude of F_i is given by $q/4\pi\epsilon|\mathbf{r}_i|^2$, where $\mathbf{r}_i$ is the vector between the ith trap and the center of the dot.

To perform the Monte Carlo simulations, a random distribution of N charge traps is created around the dot (conforming to the nanowire geometry), of which a fraction n/N are randomly selected for occupation. The calculated distribution of perturbed energies (after 10 000 simulations) for a given value of n/N is then used to calculate the linewidth for that corresponding distribution of charge traps, and we average the calculated linewidths over 1000 iterations of the calculation (i.e., 1000 random distributions of traps) in order to average out the effects of trap position. In Fig. 5 we present the calculated spectral diffusion-induced linewidth as a function of the fraction of occupied traps for several trap densities. It is clear from the figure that typical trap densities in III-nitrides (particularly $\rho = 10^{18}-10^{19}$ cm^{-3}) can easily explain power-dependent emission linewidths ranging from 100 s of μeV to a few meV, in good agreement with the experiment, and the simulation suggests that typically a few percent of the traps are occupied at any one time at the low powers used in our experiment. This average occupancy, however, is largely dependent on the number of trap states. For completeness, it is worth discussing that such a trivial model would predict a peak Γ_{SD} at $n/N = 0.5$, and that any further increase in excitation power would result in linewidth narrowing. Although our experimental conditions are far from those required to measure such a situation, the existence of a peak value for a given trap distribution can be used to rather crudely estimate the minimum density of traps in the nanowires under investigation, which we calculate to be of order 10^{17} cm^{-3}.

V. DISCUSSION

Next we briefly address the offset term from the linewidth data ($\sim 300\,\mu$eV), which is important as it shows that fluctuations in the QD environment occur even under zero optical excitation. There could be several possible origins for these fluctuations, such as thermal fluctuations in the occupancies of shallow Si dopants, or indeed residual charge migration of charge, which does not have enough energy to reenter oxygen defects (a phenomenon that has been shown to result in a persistent photocurrent in bulk AlGaN [40]). The existence of this offset imposes another limit on the degree to which spectral diffusion can be suppressed in III-nitride nanowire QDs. It may be possible, however, via extreme cooling to mK temperatures, to freeze out such fluctuations and achieve much narrower linewidths.

We note that, as very recently pointed out by Marquardt *et al.* [51], the variations in exact trap distributions from device to device will also result in slightly different emission energies between dots, even if the dots themselves have exactly the same structure. Therefore, a huge reduction in the doping densities is required for the realization of high-quality, uniform arrays of emitters. Such a reduction in dopant density may preclude the realization of efficient electrically injected devices.

VI. CONCLUDING REMARKS

Experimental characterization of the emission linewidth and spectral diffusion dynamics of single-photon-emitting

site-controlled GaN nanowire quantum dots has been performed using Fourier transform spectroscopy. By reducing the optical excitation density, the spectral diffusion could be suppressed and an estimate of the homogeneous linewidth could be made (135 μeV: consistent with results on self-assembled GaN QDs in the literature). The spectral diffusion and its characteristic excitation dependence are explained through the development of an analytical statistical model, and it is further shown that carrier trap densities consistent with donor densities in III-nitrides can explain the observed spectral diffusion via Monte Carlo analysis. Although the exciton permanent dipole moment in GaN quantum dots is large, we have shown that it is possible to suppress the spectral diffusion effects, and we have also demonstrated the existence of a zero-excitation spectral diffusion, which will place a limit on the possibility to generate indistinguishable photons. Reducing the spectral diffusion effect further in III-nitride quantum dots will be crucial for the realization of indistinguishable single-photon sources, which are required for some (though not all) QIP-related applications. Another possible method to suppress the effects of the environment would be the inclusion of nonpolar wurtzite [52] or zinc-blende [53] quantum dots in the nanowires, which should exhibit smaller permanent dipole moments.

VII. METHODS

A 266 nm wavelength continuous-wave laser (Nd:YAG fourth harmonic) is used for optical excitation in the main experiment, and it is focused at a steep angle onto the nanowire QDs that are held in a continuous-flow liquid-helium cryostat at a temperature of 4 K. The emission from individually excited QDs is collected by a 50× objective lens (NA 0.4) before being spatially filtered using a confocal pinhole and then passed to the interferometer and eventually detected on a charge-coupled device in a spectrometer with a 2400 $1\,\mathrm{mm}^{-1}$ grating. The path difference in the interferometer is tuned coarsely on μm−mm length scales using a micrometer translation stage, and fine measurements of the interference at each course step are performed by scanning on nm length scales using a piezotranslation stage. Additional measurements of the emission lifetime and the second-order coherence are performed with a pulsed frequency tripled Ti:sapphire laser ($\lambda = 256$ nm, pulse rate 80 MHz, pulse width ∼200 fs) focused onto the sample in the same way. The interferometer is bypassed during such measurements, and a Hanbury-Brown and Twiss setup consisting of two uv-enhanced photomultiplier tubes and a 50/50 beam splitter at the exit of the spectrometer is used for the photon counting.

ACKNOWLEDGMENTS

This work was supported by the Project for Developing Innovation Systems of the Ministry of Education, Culture, Sports, and Technology (MEXT), Japan. The authors acknowledge insightful discussions with S. Iwamoto and S. Sergent.

[1] A. Berthelot, I. Favero, G. Cassabois, C. Voisin, C. Delalande, P. Roussignol, R. Ferreira, and J. M. Gérard, Nat. Phys. **2**, 759 (2006).
[2] K. E. Dorfman and S. Mukamel, Sci. Rep. **4**, 3996 (2014).
[3] S. A. Empedocles, D. J. Norris, and M. G. Bawendi, Phys. Rev. Lett. **77**, 3873 (1996).
[4] S. A. Empedocles and M. G. Bawendi, Science **278**, 2114 (1997).
[5] G. Sallen, A. Tribu, T. Aichele, R. Andre, L. Besombes, C. Bougerol, M. Richard, S. Tatarenko, K. Kheng, and J. P. Poizat, Nat. Photon. **4**, 696 (2010).
[6] I. A. Ostapenko, G. Hönig, C. Kindel, S. Rodt, A. Strittmatter, A. Hoffmann, and D. Bimberg, Appl. Phys. Lett. **97**, 063103 (2010).
[7] G. Hönig, S. Rodt, G. Callsen, I. A. Ostapenko, T. Kure, A. Schliwa, C. Kindel, D. Bimberg, A. Hoffmann, S. Kako, and Y. Arakawa, Phys. Rev. B **88**, 045309 (2013).
[8] C. Kindel, S. Kako, T. Kawano, H. Oishi, Y. Arakawa, G. Honig, M. Winkelnkemper, A. Schliwa, A. Hoffmann, and D. Bimberg, Phys. Rev. B **81**, 241309 (2010).
[9] L. Zhang, T. A. Hill, C.-H. Teng, B. Demory, P.-C. Ku, and H. Deng, Phys. Rev. B **90**, 245311 (2014).
[10] R. Bardoux, T. Guillet, P. Lefebvre, T. Taliercio, T. Bretagnon, S. Rousset, B. Gil, and F. Semond, Phys. Rev. B **74**, 195319 (2006).
[11] C. Kindel, G. Callsen, S. Kako, T. Kawano, H. Oishi, G. Honig, A. Schliwa, A. Hoffmann, and Y. Arakawa, Phys. Status Solidi RRL **8**, 408 (2014).
[12] M. J. Holmes, K. Choi, S. Kako, M. Arita, and Y. Arakawa, Nano Lett. **14**, 982 (2014).
[13] S. Kako, C. Santori, K. Hoshino, S. Götzinger, Y. Yamamoto, and Y. Arakawa, Nat. Mater. **5**, 887 (2006).
[14] S. Kako, M. J. Holmes, S. Sergent, M. Bürger, D. J. As, and Y. Arakawa, Appl. Phys. Lett. **104**, 011101 (2014).
[15] S. Deshpande, T. Frost, A. Hazari, and P. Bhattacharya, Appl. Phys. Lett. **105**, 141109 (2014).
[16] S. Kremling, C. Tessarek, H. Dartsch, S. Figge, S. Höfling, L. Worschech, C. Kruse, D. Hommel, and A. Forchel, Appl. Phys. Lett. **100**, 061115 (2012).
[17] L. Zhang, C.-H. Teng, T. A. Hill, L.-K. Lee, P.-C. Ku, and H. Deng, Appl. Phys. Lett. **103**, 192114 (2013).
[18] Y. Huang, X. Duan, Y. Cui, and C. M. Lieber, Nano Lett. **2**, 101 (2002).
[19] T. Nakaoka, S. Kako, Y. Arakawa, and S. Tarucha, Appl. Phys. Lett. **90**, 162109 (2007).
[20] Y.-J. Lu, C.-Y. Wang, J. Kim, H.-Y. Chen, M.-Y. Lu, Y.-C. Chen, W.-H. Chang, L.-J. Chen, M. I. Stockman, C.-K. Shih, and S. Gwo, Nano Lett. **14**, 4381 (2014).
[21] G. Christmann, R. Butté, E. Feltin, J.-F. Carlin, and N. Grandjean, Appl. Phys. Lett. **93**, 051102 (2008).
[22] J. Heo, S. Jahangir, B. Xiao, and P. Bhattacharya, Nano Lett. **13**, 2376 (2013).
[23] A. Woolf, T. Puchtler, I. Aharonovich, T. Zhu, N. Niu, D. Wang, R. Oliver, and E. L. Hu, Proc. Natl. Acad. Sci. USA **111**, 14042 (2014).

[24] I. Aharonovich, A. Woolf, K. J. Russell, T. Zhu, N. Niu, M. J. Kappers, R. A. Oliver, and E. L. Hu, Appl. Phys. Lett. **103**, 021112 (2013).
[25] S. De Rinaldis, I. D'Amico, E. Biolatti, R. Rinaldi, R. Cingolani, and F. Rossi, Phys. Rev. B **65**, 081309 (2002).
[26] S. Tomić, J. Pal, M. A. Migliorato, R. J. Young, and N. Vukmirović, ACS Photon. **2**, 958 (2015).
[27] K. Choi, S. Kako, M. J. Holmes, M. Arita, and Y. Arakawa, Appl. Phys. Lett. **103**, 171907 (2013).
[28] K. Choi, M. Arita, S. Kako, and Y. Arakawa, J. Cryst. Growth **370**, 328 (2013).
[29] M. J. Holmes, S. Kako, K. Choi, P. Podemski, M. Arita, and Y. Arakawa, Phys. Rev. Lett. **111**, 057401 (2013).
[30] M. J. Holmes, S. Kako, K. Choi, P. Podemski, M. Arita, and Y. Arakawa, Nano Lett. **15**, 1047 (2015).
[31] C. Kammerer, G. Cassabois, C. Voisin, M. Perrin, C. Delalande, P. Roussignol, and J. M. Gérard, Appl. Phys. Lett. **81**, 2737 (2002).
[32] V. Zwiller, T. Aichele, and O. Benson, Phys. Rev. B **69**, 165307 (2004).
[33] T. Kuroda, Y. Sakuma, K. Sakoda, K. Takemoto, and T. Usuki, Appl. Phys. Lett. **91**, 223113 (2007).
[34] H. Kamada and T. Kutsuwa, Phys. Rev. B **78**, 155324 (2008).
[35] S. Kako, M. Miyamura, K. Tachibana, K. Hoshino, and Y. Arakawa, Appl. Phys. Lett. **83**, 984 (2003).
[36] L. Besombes, K. Kheng, L. Marsal, and H. Mariette, Phys. Rev. B **63**, 155307 (2001).
[37] P. Borri, W. Langbein, S. Schneider, U. Woggon, R. L. Sellin, D. Ouyang, and D. Bimberg, Phys. Rev. Lett. **87**, 157401 (2001).
[38] F. Demangeot, D. Simeonov, A. Dussaigne, R. Butté, and N. Grandjean, Phys. Status Solidi C **6**, S598 (2009).
[39] S. A. Empedocles and M. G. Bawendi, J. Phys. Chem. B **103**, 1826 (1999).
[40] M. D. McCluskey, N. M. Johnson, C. G. Van de Walle, D. P. Bour, M. Kneissl, and W. Walukiewicz, Phys. Rev. Lett. **80**, 4008 (1998).
[41] T. Onuma, S. Chichibu, A. Uedono, T. Sota, P. Cantu, T. M. Katona, J. F. Keading, S. Keller, U. K. MIshra, S. Nakamura, and S. P. Denbaars, J. Appl. Phys. **95**, 2495 (2004).
[42] R. Calarco, M. Marso, T. Richter, A. I. Aykanat, R. Meijers, A. von d Hart, T. Stoica, and H. Lüth, Nano Lett. **5**, 981 (2005).
[43] D. Camacho Mojica and Y.-M. Niquet, Phys. Rev. B **81**, 195313 (2010).
[44] Y. M. Bishop, S. E. Fienberg, and P. W. Holland, *Discrete Multivariate Analysis: Theory and Practice* (Springer, New York, 2007).
[45] M. L. Nakarmi, N. Nepal, J. Y. Lin, and H. X. Jiang, Appl. Phys. Lett. **86**, 261902 (2005).
[46] C. G. Van de Walle, Phys. Rev. B **57**, R2033 (1998).
[47] K. B. Nam, M. L. Nakarmi, J. Y. Lin, and H. X. Jiang, Appl. Phys. Lett. **86**, 222108 (2005).
[48] J. Oila, J. Kivioja, V. Ranki, K. Saarinen, D. C. Look, R. J. Molnar, S. S. Park, S. K. Lee, and J. Y. Han, Appl. Phys. Lett. **82**, 3433 (2003).
[49] A. Calloni, R. Ferragut, A. Dupasquier, H. von Känel, A. Guiller, A. Rutz, L. Ravelli, and W. Egger, J. Appl. Phys. **112**, 024510 (2012).
[50] S. Birner, T. Zibold, T. Andlauer, T. Kubis, M. Sabathil, A. Trellakis, and P. Vogl, IEEE Trans. Electron Dev. **54**, 2137 (2007).
[51] O. Marquardt, L. Geelhaar, and O. Brandt, Nano Lett. **15**, 4289 (2015).
[52] B. P. L. Reid, C. Kocher, T. Zhu, F. Oehler, C. C. S. Chan, R. A. Oliver, and R. A. Taylor, Appl. Phys. Lett. **106**, 171108 (2015).
[53] S. Sergent, S. Kako, M. Bürger, T. Schupp, D. J. As, and Y. Arakawa, Phys. Rev. B **90**, 235312 (2014).